

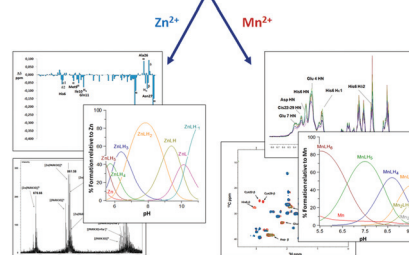
1

## Manganism and Parkinson's disease: Mn(II) and Zn(II) interaction with a 30-amino acid fragment

Maurizio Remelli,\* Massimiliano Peana,  
Serenella Medici, Malgorzata Ostrowska,  
Elzbieta Gumienna-Kontecka and  
Maria Antonietta Zoroddu\*

A protected 30-amino acid fragment, **Acetyl-SPDEKHELMIQQLKLDYTVGFCGDGANDCG-Amide**, **Acetyl-Ser-Pro-Asp-Glu-Lys-His-Glu-Leu-Met-Ile-Gln-Leu-Gln-Lys-Leu-Asp-Tyr-Thr-Val-Gly-Phe-Cys-Gly-Asp-Gly-Ala-Asn-Asp-Cys-Gly-Amide**, encompassing the sequence from residues **1165** to 1193 in the encoded protein from Parkinson's disease gene Park9 (YPk9), was studied for manganese and zinc binding.

from residues 1165 to 1193 in the encoded protein from Parkinson's disease gene Park9 (YPk9)  
Ac-SPDEKHELMIQQLKLDYTVGFCGDGANDCG-Am



Q3

Please check this proof carefully. **Our staff will not read it in detail after you have returned it.**

Translation errors between word-processor files and typesetting systems can occur so the whole proof needs to be read. Please pay particular attention to: tabulated material; equations; numerical data; figures and graphics; and references. If you have not already indicated the corresponding author(s) please mark their name(s) with an asterisk. Please e-mail a list of corrections or the PDF with electronic notes attached – do not change the text within the PDF file or send a revised manuscript. Corrections at this stage should be minor and not involve extensive changes. All corrections must be sent at the same time.

**Please bear in mind that minor layout improvements, e.g. in line breaking, table widths and graphic placement, are routinely applied to the final version.**

We will publish articles on the web as soon as possible after receiving your corrections; **no late corrections will be made.**

Please return your **final** corrections, where possible within **48 hours** of receipt, by e-mail to: dalton@rsc.org

## Queries for the attention of the authors

Journal: **Dalton Transactions**

Paper: **c6dt00184j**

Title: **Manganism and Parkinson's disease: Mn(II) and Zn(II) interaction with a 30-amino acid fragment**

Editor's queries are marked like this [Q1, Q2, ...], and for your convenience line numbers are indicated like this [5, 10, 15, ...].

Please ensure that all queries are answered when returning your proof corrections so that publication of your article is not delayed.

Query Reference	Query	Remarks
Q1	For your information: You can cite this article before you receive notification of the page numbers by using the following format: (authors), Dalton Trans., (year), DOI: 10.1039/c6dt00184j.	
Q2	Please carefully check the spelling of all author names. This is important for the correct indexing and future citation of your article. No late corrections can be made.	
Q3	The first line of the Abstract has been inserted as the Graphical Abstract text. Please check that this is suitable. If the text does not fit within the two horizontal lines, please trim the text and/or the title.	
Q4	Ref. 28: Please provide the title.	

## Manganism and Parkinson's disease: Mn(II) and Zn(II) interaction with a 30-amino acid fragment†

Cite this: DOI: 10.1039/c6dt00184j

Maurizio Remelli,<sup>\*a</sup> Massimiliano Peana,<sup>b</sup> Serenella Medici,<sup>b</sup> Malgorzata Ostrowska,<sup>c</sup> Elzbieta Gumienka-Kontecka<sup>c</sup> and Maria Antonietta Zoroddu<sup>\*b</sup>

A protected 30-amino acid fragment, Acetyl-SPDEKHELMIQQLDLYTVGFCGDGANDCG-Amide, Acetyl-Ser-Pro-Asp-Glu-Lys-His-Glu-Leu-Met-Ile-Gln-Leu-Gln-Lys-Leu-Asp-Tyr-Thr-Val-Gly-Phe-Cys-Gly-Asp-Gly-Ala-Asn-Asp-Cys-Gly-Amide, encompassing the sequence from residues 1165 to 1193 in the encoded protein from Parkinson's disease gene Park9 (YPk9), was studied for manganese and zinc binding. Manganese exposure is considered to be an environmental risk factor connected to PD and PD-like syndrome. Research into the genetic and environmental risk factors involved in disease susceptibility has recently uncovered a link existing between Park9 and manganese. It seems that manganese binding to Park9 (YPk9) protein is involved in the detoxification mechanism exerted by this protein against manganese toxicity. In this study, we used potentiometric, mono- and bi-dimensional TOCSY, HSQC NMR, EPR and ESI-MS measurements to analyze complex formation and metal binding sites in the peptide fragment. Presumably octahedral species, in which the Mn(II) ion was bound to oxygens of the carboxyl groups of Glu and Asp, and species where the involvement of sulfur from Cys and nitrogen from His residues, depending on the metal to ligand molar ratio, were detected for manganese coordination. Structural changes in the 30-amino acid fragment were triggered by Zn(II) interaction. A general decrease in the intensity of NMR signals was detected, suggesting the occurrence of chemical exchange among some coordinated species in an intermediate NMR timescale. The coordination may involve both S and N donor atoms from cysteine as well as histidine residues, together with O donor atoms from glutamic and aspartic residues. **No bis-complexes and only mono-complexes were detected throughout the pH range for both metal ions.**

Received 14th January 2016,

Accepted 3rd February 2016

DOI: 10.1039/c6dt00184j

www.rsc.org/dalton

## Introduction

Manganese is an essential trace metal for humans.<sup>1</sup> Exposure to high concentrations of manganese, also in the form of nanoparticles,<sup>2</sup> can cause toxic effects that are detrimental to human health.<sup>3</sup> There is sufficient evidence in the literature of neurodegenerative effects at a concentration of manganese lower than 0.2 mg m<sup>-3</sup> in inhaled air.<sup>4,5</sup> However, the effective doses inhaled by exposed workers are much higher and are thus cause of major concern.

In particular, neurological symptoms attributable to high levels of manganese exposure share many features with Parkinson's disease (PD).<sup>6–8</sup>

It has been well established that PD is far more common in industrial areas where manganese emission levels are high, suggesting a possible link between PD and manganese exposure. In fact, welders, steel workers and miners exposed to manganese inhalation are at high risk of developing Parkinson-like syndromes known as manganism or manganese poisoning.<sup>6,9</sup>

It has been shown that a member of the ATPase family (P5-type), the human gene Park9 and its yeast homologue YPk9, can protect cells against manganese toxicity. By deleting the YPk9 gene from yeast cells, they remain viable but, after exposure to manganese, they could no longer survive, differently from the exposure to other metal ions, such as zinc or copper.<sup>10</sup>

Within this context, it is important to mention that the location of YPk9 protein in yeast cells resides within the vacuole, a bag which captures toxins, suggesting that the protein is capable of taking in toxic metal ions.

In particular, the selective sensitivity of mutant cells to manganese ions suggests that the protein is a metal sequestering protein capable of preventing manganese poisoning.<sup>10</sup>

Thus, in our search for the mechanism by which Park9 (YPk9) confers protection to PD and for a possible correlation of the disease with a combination of both genetic and environ-

<sup>a</sup>Department of Chemical and Pharmaceutical Sciences, University of Ferrara, Italy.  
E-mail: rmm@unife.it

<sup>b</sup>Department of Chemistry and Pharmacy, University of Sassari, Italy.  
E-mail: zoroddu@uniss.it

<sup>c</sup>Faculty of Chemistry, University of Wrocław, Poland

† Electronic supplementary information (ESI) available. See DOI: 10.1039/c6dt00184j

mental factors, we focused our attention on some of the promising highly conserved sequences of Park9 and Ypk9 for ion binding. In particular, we studied a 30-amino acid (30-aa) fragment encompassing the sequence from residues 1165 to 1193 in the encoded protein from Parkinson's disease gene for manganese and zinc binding. These two metals, the paramagnetic Mn(II) and the diamagnetic Zn(II) ion, can offer a viewpoint on the coordination ability of the fragment.

In previous reports,<sup>11,12</sup> we described the interaction of Mn(II) and Zn(II) ions with two partial portions (the monohistidinic PK9-H and biscysteinic PK9-C peptides) of the 30-aa fragment.

Here, we present a study on the entire Ac-SPDEKHELMIQ-LQKLDYTVGFCGDGANDCG-Am, N- and C-terminal respectively acetylated and amidated fragments. Alongside a histidine and two cysteines, this fragment includes six oxygen donor amino acid residues which through their oxygen donors could have an important role in the homeostasis of Mn(II) ions regarding both its transport and, eventually, its detoxification mechanisms.

The histidine in the 6<sup>th</sup> position and the two cysteine residues, in the 22<sup>nd</sup> and 29<sup>th</sup> positions, surrounded by several aspartic and glutamic acid residues which can complete the coordination sphere, can presumably act as the anchoring sites for metal ions.

The study was performed using potentiometric titration and NMR, EPR and ESI-MS techniques.

Potentiometric titrations allowed us to determine the stoichiometry and the stability constants of the observable species together with the pH dependent deprotonation steps of the studied peptide; spectroscopic techniques allowed us to support and confirm the potentiometric results and to identify the binding donor atoms involved in the coordination process.

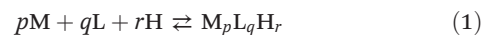
## Experimental

### Potentiometric measurements

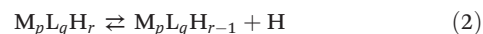
Potentiometric titrations were performed with the following apparatus: Orion EA 940 and Orion 720A pH meters (resolution 0.1 mV, accuracy 0.2 mV) equipped with a combined glass electrode (Metrohm EA125); Hamilton MicroLab M and MicroLab300 motor burettes (resolution 0.1  $\mu$ l, accuracy 0.2  $\mu$ l) equipped with Hamilton syringes (delivery volume 250 and 500  $\mu$ l, respectively). Constant-speed magnetic-stirring was applied throughout. The temperature of the titration cell was maintained at 298.2  $\pm$  0.1 K by using a Haake F3C circulation thermostat. UPP grade nitrogen, previously saturated with H<sub>2</sub>O (bubbling into a solution of KCl 0.1 M, at 298.2 K) was gently blown over the test solution in order to maintain an inert atmosphere. The electrode couple was standardized on the pH =  $-\log c_{\text{H}^+}$  scale by titration of HCl (0.01 M) with standard KOH at 298.2 K and  $I = 0.1$  M (KCl). Aliquots (2 ml) of the sample solution, containing suitable amounts of metal, ligand, HCl and KCl, were first titrated with standard KOH and then back-titrated with standard HCl, without opening the

reaction vessel, in order to check the reversibility of the metal-complex formation reactions. The concentration range employed for the metal ions was 0.5–1.0 mM with a metal to ligand molar ratio of about 1:1.1. The Hyperquad program<sup>13</sup> was used for stability constant calculations and their standard deviations, which represent random errors only. The speciation and competition diagrams were plotted using the Hyss program.<sup>14</sup>

Reported  $\log \beta$  values refer to the overall complex-formation equilibrium:



while  $pK_a$  values refer to the proton dissociation process:



(charges omitted;  $p$  might also be 0 and  $r$  can be negative).

The stability constants of the complexes with different stoichiometry and protonation degrees cannot be directly compared. The most popular parameters used to compare the global binding ability of a ligand towards two or more metal ions, under given experimental conditions (*i.e.* at physiological pH) are the dissociation constant ( $K_d$ )<sup>15</sup> and the  $pM$  value.<sup>16</sup> The former refers to a hypothetical overall equilibrium:



where the protonation degree of the ligand (and the complex) is not explicitly considered. The second parameter is the negative logarithm of the concentration of the free metal ion ( $pM$ ), in the presence of the ligand, under normalized experimental conditions, *i.e.*  $[L]_{\text{total}} = 10^{-5}$  M and  $[M]_{\text{total}} = 10^{-6}$  M, at pH 7.4. In addition, the comparison can be extended to the whole explored pH range by computing and plotting the "competition diagrams". These plots refer to hypothetical solutions where both the ligand and two types of metal ions are present at the same time in solution under given experimental conditions (generally, equimolar concentrations are considered). Competition plots are calculated by means of the speciation models obtained by potentiometry, assuming that no mixed-ligand species is formed.

### EPR spectroscopy

Electron paramagnetic resonance (EPR) spectra were recorded using a Bruker ELEXSYS E500 CW-EPR spectrometer equipped with an NMR teslameter (ER 036TM) and a frequency counter (E 41 FC) at X-band frequency, at 77 K and room temperature. The concentration of peptide was 1 mM and the metal to ligand molar ratio was 1:1.2. The solution for EPR was prepared with ethylene glycol (5%) as a cryoprotectant. The EPR parameters were obtained by the simulation of plots using the Bruker WinEPR SimFonia program and the Doubletnew (EPR OF  $S = 1/2$ ) program by Dr Andrew Ozarowski, National High Field Magnetic Laboratory, University of Florida.

### Electrospray ionization-mass spectrometry (ESI-MS)

Electrospray ionization mass spectrometry (ESI-MS) data were collected using a BrukerMicro-TOF-Q spectrometer (Bruker

Daltonik, Bremen, Germany), equipped with an Apollo II electrospray ionization source with an ion funnel. The spectra were recorded in the positive and negative ion modes in the range 100 to 1500  $m/z$ . The instrumental parameters were as follows: scan range  $m/z$  400–1600, dry gas–nitrogen, temperature 170 °C, and ion energy 5 eV. The capillary voltage was optimized to the highest S/N ratio and it was 4500 V. The small changes in the voltage ( $\pm 500$  V) did not significantly affect the optimized spectra. Samples (with metal to ligand 1 : 1.2 stoichiometry, and [ligand] =  $10^{-5}$  M) were prepared by using a MeOH/H<sub>2</sub>O mixture (50/50 v/v) as a solvent, at pH 7.4 and 9.0. The instrument was calibrated using the Tunemix mixture (Bruker Daltonik, Germany) in the quadratic regression mode. The overall charge of the analyzed ions was calculated on the basis of the distance between isotopic peaks. Data were processed by the application of the Compass DataAnalysis 4.0 (Bruker Daltonik, Germany) program.

### NMR spectroscopy

NMR measurements were performed on a Bruker Ascend™ 400 MHz spectrometer equipped with a 5 mm automated tuning and matching broad band probe (BBFO) with  $z$ -gradients, as previously described.<sup>17–22</sup>

NMR experiments were carried out using 5 mM concentration of the ligands in 90/10 (v/v) H<sub>2</sub>O/D<sub>2</sub>O at 298 K in 5 mm NMR tubes. 2D <sup>1</sup>H–<sup>13</sup>C heteronuclear correlation spectra (HSQC) were recorded using a phase-sensitive sequence employing an Echo-Antiecho-TPPI gradient selection with a heteronuclear coupling constant  $J_{\text{XH}} = 145$  Hz, and shaped pulses for all 180° pulses on a  $f_2$  channel with decoupling during acquisition. Sensitivity improvement and gradients in back-incept were also used. Relaxation delays of 2 s and 90° pulses of about 10  $\mu$ s were employed in all the experiments. Solvent suppression for 1D <sup>1</sup>H and 2D <sup>1</sup>H–<sup>1</sup>H TOCSY (total correlation spectroscopy) experiments was carried out by using excitation sculpting with gradients. The spin-lock mixing time of TOCSY experiments was obtained with MLEV17. <sup>1</sup>H–<sup>1</sup>H TOCSY spectra were recorded using mixing times of 60 ms. A combination of 1D, 2D TOCSY, and HSQC experiments was used to assign the signals of both free and metal-bound ligands at different pH values. All NMR data were processed with TopSpin (Bruker Instruments) software and analyzed by Sparky 3.11 and MestRe Nova 6.0.2 (Mestrelab Research S.L.) programs.

### Model calculations

A model for Ypk9 protein was built by using the ESyPred3D automated homology modelling program.<sup>23</sup> The 3D X-ray structure of the sodium–potassium pump protein (PDB 3B8E),<sup>24</sup> which shares 23.0% of identities and 17.0% of similarities with the Ypk9 sequence, was used as a template in the modeling.<sup>11</sup>

The model of Park30 peptide, SPDEKHELMIQKL-DYTVGFCGDGANDCG, was then generated from the obtained predicted structure. Mn(II) coordination with the Park30 fragment was modeled, according to the spectroscopic results, as

previously described,<sup>11,25</sup> using the molecular mechanics geometry optimizations obtained by an AMBER force field implemented in HyperChem™ 8.0.7 molecular modeling software. Molecular graphics of the most likely coordination sphere for Mn(II) species at different pH values, were generated by using the UCSF-Chimera package.<sup>26</sup>

## Results and discussion

### Protonation equilibria

Park30 contains twelve amino acids involved in acid–base equilibria. Nine of them can be classified as weak acids, in that they can release a proton (four Asp, two Glu, two Cys and one Tyr residues); the other three amino acids can be classified as weak bases, since they may accept a proton (two Lys and one His residues). The hydrogens bound to the amide nitrogens of the polypeptide chain have a  $pK_a$  value of nearly 15 (ref. 27) and, in the absence of metal ions able to displace them, cannot be considered exchangeable. Therefore, the completely deprotonated ligand bears nine negative charges ( $L^{9-}$ ). The overall protonation constants ( $\log \beta$ ) and the corresponding dissociation step-values ( $pK_a$ ) for Park30 are reported in Table 1 while a representative distribution diagram as a function of pH is given in Fig. 1.

The potentiometric results of Table 1 refer to five titrations carried out either with HCl or NaOH, between pH 6.0 and pH 11 (approximately 200 points,  $\sigma = 0.7$ ). The lower pH value was imposed by the solubility of Park30 and the first species can most likely be attributed to the neutral species LH<sub>0</sub>, that begins to form around pH 6.0. This prevented us from determining the  $pK_a$  values of aspartic acid residues which are deprotonated throughout the explored pH range. However, these  $pK_a$  values are irrelevant in the determination of complex-formation constants.

Indeed, Glu residues are less acidic than Asp residues and the  $pK_a$  of glutamic acid is significantly higher than that of aspartic acid due to the inductive effect of the additional methylene group, as reported in the literature.<sup>28</sup>

**Table 1** Protonation constants for Park30, at  $T = 298$  K and  $I = 0.1$  mol dm<sup>-3</sup> (KCl)

	$\log \beta$	$pK_a$	Residue
LH <sup>8-</sup>	10.47(5)	10.47	K
LH <sub>2</sub> <sup>7-</sup>	20.84(2)	10.37	K
LH <sub>3</sub> <sup>6-</sup>	30.36(6)	9.52	Y
LH <sub>4</sub> <sup>5-</sup>	39.52(4)	9.16	C
LH <sub>5</sub> <sup>4-</sup>	47.96(8)	8.44	C
LH <sub>6</sub> <sup>3-</sup>	54.8(1)	6.8	H
LH <sub>7</sub> <sup>2-</sup>	60.7(2)	5.9	E
LH <sub>8</sub> <sup>-</sup>	(65.7) <sup>a</sup>	(5.0) <sup>a</sup>	E
LH <sub>9</sub>	—	—	D
LH <sub>10</sub> <sup>+</sup>	—	—	D
LH <sub>11</sub> <sup>2+</sup>	—	—	D
LH <sub>12</sub> <sup>3+</sup>	—	—	D

<sup>a</sup> Tentative value.



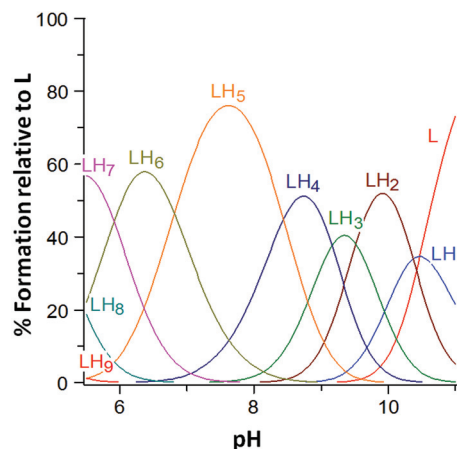


Fig. 1 Representative distribution diagram for the protonation equilibria of Park30;  $C_L^{\circ} = 1 \times 10^{-3} \text{ mol dm}^{-3}$ .

The two lysines and tyrosine are certainly the most basic residues of Park30. The two highest  $pK_a$  values (10.47 and 10.37) could be ascribed to Lys residues. **These two lysines were practically identical, as expected,** considering that they are quite far apart from each other for which protonation should be almost simultaneous. The Tyr residue was then characterized by a  $pK_a$  value of 9.52, in agreement with what has been reported in the literature for peptides containing this amino acid.<sup>29</sup>

Further down the scale of alkalinity, the two cysteines had  $pK_a$  values of 9.16 and 8.44, respectively, only slightly lower than those found for the shorter fragment Ac-FCGDGANDCG-Am (PK9-C; 9.35 and 8.59<sup>12</sup>). The protonation constant (6.8) of the histidyl residue was identical to that of the shorter fragment Ac-PDEKHEL-Am (PK9-H; 6.81<sup>12</sup>), corresponding to the amino-terminal sequence of Park30.

Finally, the protonation constants of the two glutamic sites were about one order of magnitude higher than those of PK9-H (*i.e.* the sites within the Park30 fragment are less acidic). This feature can be attributed to the different charges of the two peptides. In fact, in the case of Park30, the first glutamic proton is released from the negative species  $LH_8^-$ , while for PK9-H the corresponding species is positively charged ( $LH_4^+$ ). The same applies to the second glutamic proton (from  $LH_7^{2-}$  for Park30 and instead from the neutral  $LH_3$  species in the case of PK9-H). In other words, the release of both protons is disfavored by the negative charge of Park30 and therefore the residues are weaker acids.

When comparing the NMR spectra of the free ligand obtained at pH 6.1 with those obtained at pH 7.3, no overt changes in chemical shifts were observed in the aliphatic region except for the  $H\beta$  protons of the histidine residue. Also protons of aspartate and glutamate did not change their chemical shift, supporting that, in this range of pH, they are already deprotonated as suggested by potentiometric data.

Conversely, changes in chemical shifts were observed in the aromatic region for  $H\epsilon$  and  $H\delta$  of histidine residue and for

several amidic NH protons from the backbone of the peptide. Fig. 2 shows the results obtained within the aromatic region of TOCSY spectra. Major changes were detectable for  $H\delta_2$  from histidine,  $H_N$  from glutamic Glu7 and to a lesser extent from Glu4 residues, as well as for protons from aspartic, glycine and glutamine residues.

It was not possible to distinguish the specific aspartic or glutamic residue affected by deprotonation because they all overlapped in the spectrum. The overt change in the chemical shift of the cross-correlation involving  $H\beta-H_N$  and  $H\beta-\delta_2$  of histidine residue, which is in the 6<sup>th</sup> position, coupled to the concomitant variation of chemical shift of the cross-peaks  $H\alpha-H_N$ ,  $H\beta-H_N$ , and  $H\gamma-H_N$  of the close residue Glu7, is in agreement with the potentiometric measurements and shows that histidine starts to undergo deprotonation within this pH range (Fig. 2).

Fig. 3a and b show the comparison of the chemical shifts observed for the peptide within HSQC spectra. At a glance, it is possible to follow the deprotonation steps occurring by changing the pH. From pH 6.1 to pH 8.6, variations in the chemical shifts of  $H\epsilon_1$  and  $H\delta_2$  protons from histidine are clearly visible; the variation involving  $H\epsilon_1$  was more pronounced.

When the pH value was raised from 8.6 to 9.5, variations in chemical shifts involved cysteine protons, as well as  $H\beta$  protons of the histidine side chain and  $H\epsilon$  protons of tyrosine. Weak changes were also observed for  $H\epsilon$  and  $H\delta$  of lysines, Lys5 and 14 and  $H\delta$  of tyrosine.

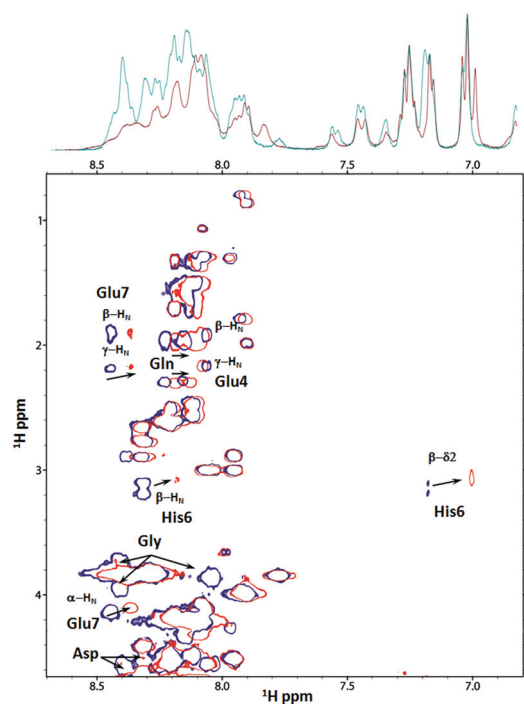


Fig. 2 Selection of the aromatic region in the  $^1\text{H}-^1\text{H}$  TOCSY NMR spectra for Park30 peptide, at pH 6.1 (blue) and pH 7.3 (red). The largest proton chemical shift changes have been labeled.

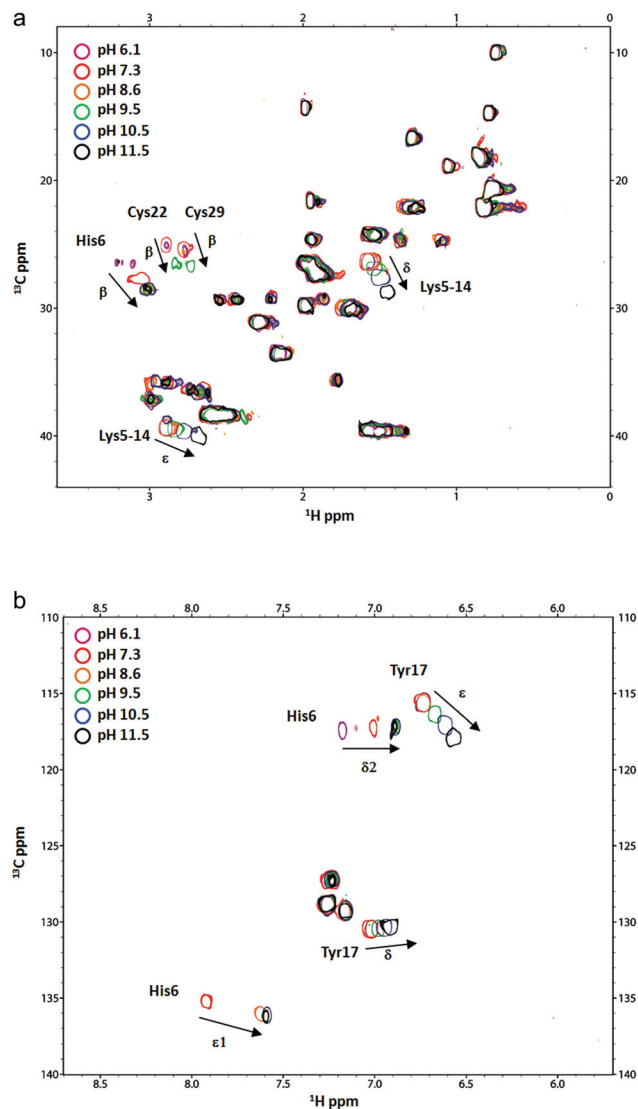


Fig. 3 a, b. Selection of aliphatic and aromatic regions in the  $^{13}\text{C}$ - $^1\text{H}$  HSQC NMR spectra for Park30 peptide at different pH values. The largest C-H correlation chemical shift changes have been labeled.

From pH 8.6 to 11.5 more pronounced changes in the chemical shifts of tyrosine signals were observed for  $\delta$  and  $\epsilon$  protons, particularly for He. From pH 9.5 onwards, He and H $\delta$  signals derived from the side chains of lysine residues Lys5-14 were also strongly affected. It was not possible to distinguish between Lys5 and Lys14 residues in the NMR spectra.

It is likely that, according to potentiometric measurements, the last two deprotonations involved tyrosine and lysine residues.

### Mn(II) complexes

The potentiometric results were obtained from three titrations carried out either with HCl or NaOH in the pH range 5.5-9.5 (about 50 points,  $\sigma = 3.1$ ). The lower pH limit was dictated by the solubility of the ligand and the upper limit by the oxidation of Mn(II) in the basic medium. The complex-formation

Table 2 Complex-formation constants for the system Mn(II)/Park30, at  $T = 298\text{ K}$  and  $I = 0.1\text{ mol dm}^{-3}$  (KCl)

	$\log \beta$	$\text{p}K_{\text{a}}$
$[\text{MnLH}_6]^-$	60.3(1)	6.7
$[\text{MnLH}_5]^{2-}$	53.6(1)	8.3
$[\text{MnLH}_4]^{3-}$	45.3(1)	9.2
$[\text{MnLH}_3]^{4-}$	36.1(1)	
$[\text{Mn}_2\text{LH}_2]^{3-}$	31(1)	

constants are reported in Table 2; in Fig. 4a a representative distribution diagram for the system Mn(II)/Park30 is shown.

The speciation model of Table 2 contains four complexes with stoichiometry 1 : 1 and with different degrees of protonation, along with the binuclear species  $[\text{Mn}_2\text{LH}_2]^{3-}$  that forms at basic pH in non-negligible percentages. Despite that under our experimental conditions the peptide is always in slight excess with respect to the metal, it was not possible to insert any bis-complexes within the model.

At pH 5.5, already more than 80% of manganese is complexed by Park30 and the percentage of free metal ions slowly decreases as the pH increases and the complex loses protons. Given the abundance of donor atoms in the ligand, many combinations are possible. However, some factors need to be considered: (i) at pH 5.5 (or higher) the carboxyl groups of aspartic acids and, at least partially, of glutamic acids are deprotonated; (ii) the stoichiometry of the most abundant complex at pH 5.5,  $[\text{MnLH}_6]^-$ , indicates that six residues of the peptide are protonated; (iii) the three  $\text{p}K_{\text{a}}$  values corresponding to the subsequent deprotonation steps are virtually identical to those measured for His and the two Cys, in the absence of metal; (iv) the deprotonation of the other three, more basic, sites (Tyr, Lys, and Lys) requires instead pH values higher than those explored here. All these considerations seem to converge on a structural hypothesis for the complex  $[\text{MnLH}_6]^-$ , presumably octahedral, in which the Mn(II) ion is bound to the

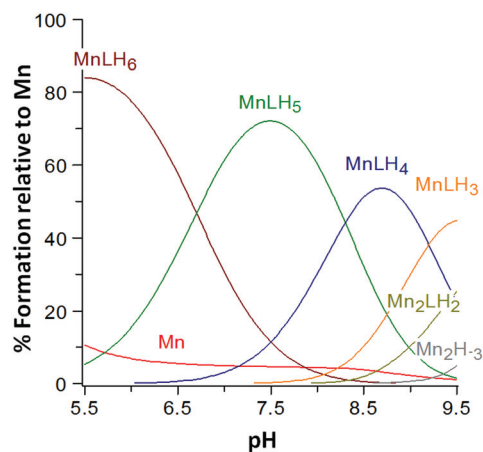


Fig. 4 Representative distribution diagram for the complex-formation equilibria in the system Mn(II)/Park30;  $C_{\text{L}} = 1 \times 10^{-3}\text{ mol dm}^{-3}$ ;  $M/L$  ratio = 1 : 1.

oxygen atoms of the carboxylate groups of the peptide and possibly also to some water molecules.<sup>30</sup>

With increasing pH from pH 6 onwards, the imidazole protons of histidine and the two thiol groups of cysteines are gradually released. Finally, at alkaline pH, a second metal ion can be bound by Park30, to form the binuclear species  $[\text{Mn}_2\text{LH}_2]^{3-}$ . The stoichiometry of this species requires that also tyrosine is deprotonated but it is not possible to state whether its phenolic group takes part in the formation of the binuclear complex.

Interaction of the Mn(II) ion was investigated by using the mono- and bi-dimensional NMR technique to follow and evaluate the selective paramagnetic broadening or shift effects expected upon metal binding. NMR has been performed employing a substoichiometric amount of manganese ions. Within a range of pH 6 to 6.6 and at a Mn(II) to peptide molar ratio of 0.02 : 1, in the HSQC and TOCSY spectra the disappearance of the C–H and H–H correlations from Cys22 and 29, respectively has been clearly detected. In addition, the selective disappearance of the alanine spin system, the alanine located in the 26<sup>th</sup> position between the two cysteines, supports the involvement of cysteines as the anchoring sites for Mn(II) ions in this condition. Histidine signals do not appear to be affected upon addition of manganese at this pH and the metal to ligand molar ratio.

At pH 7 also the protons from histidine undergo changes by the disappearance of C–H correlation in the HSQC spectra, showing its concomitant participation together with cysteines in the coordination with Mn(II) ions (Fig. 5).

By raising the Mn(II) to peptide molar ratio from 0.02 : 1 to 0.2 : 1, it is possible to note that within the HSQC spectra obtained at pH 7.3 (Fig. 6a and b) a selective and simultaneous disappearance of H $\epsilon$ , H $\delta$  and H $\beta$  from His, H $\beta$  from Cys22 and Cys29 together with a selective disappearance of spin corre-

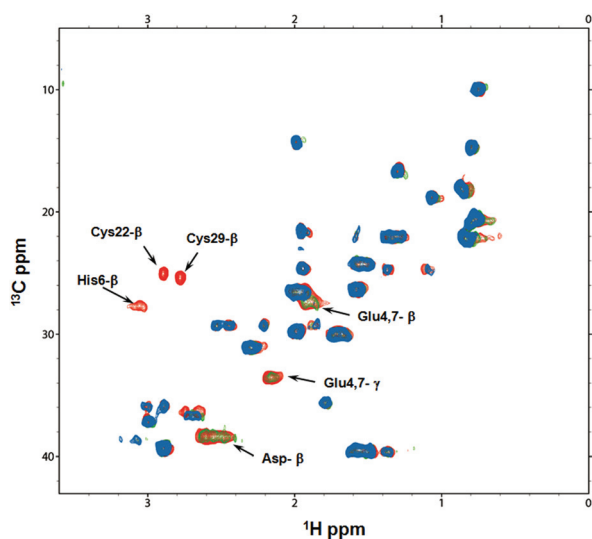


Fig. 5 Selection of the aliphatic region in the  $^{13}\text{C}$ - $^1\text{H}$  HSQC NMR spectra for Park30 peptide, in the absence (red) and in the presence of 0.02 (green) and 0.2 (blue) equivalent of Mn(II), at pH 7.3.

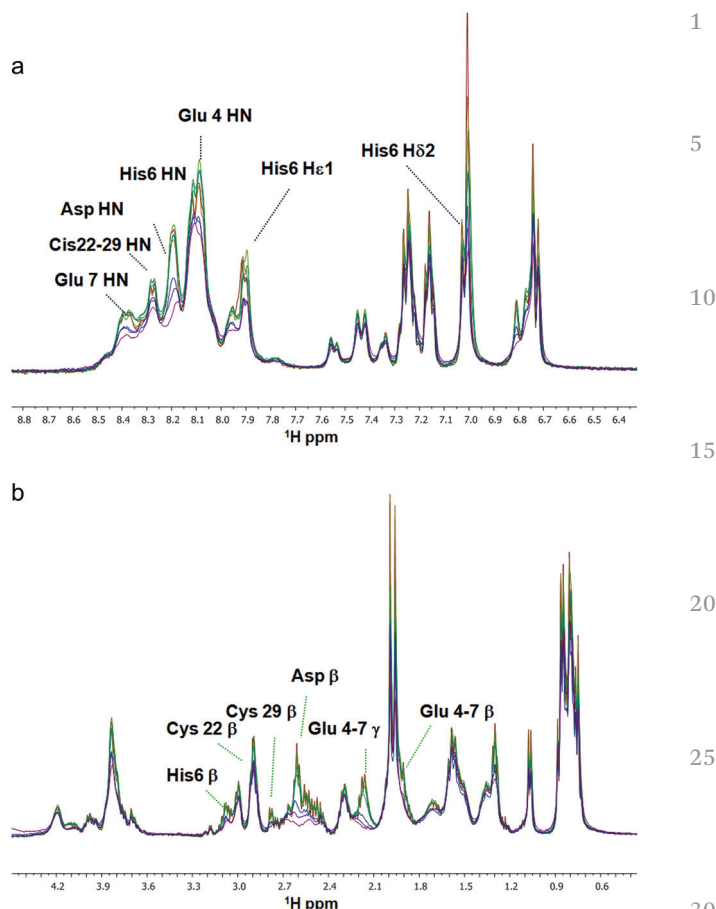


Fig. 6 Superimposition of  $^1\text{H}$  NMR spectra for Park30 peptide, at pH 7.3, by increasing the metal to ligand molar ratio from 0.02 : 1 to 0.2 : 1.

lations from Glu4–7 and Asp residues, which highlights that also these residues can be involved in the coordination; for Asp residues it was not possible to identify the specific residue involved being all together overlapped though.

The circumstances under which cysteines can be involved in the coordination is also supported by the selective disappearance, or strong loss in intensity, of the signals from the residues in the 17<sup>th</sup>, 21<sup>st</sup>, 26<sup>th</sup> and 27<sup>th</sup> positions, of Tyr, Phe, Ala and Asn, respectively located towards the C-terminus of the fragment where the cysteine residues are placed, which can probably be the result of changes in the conformation of the backbone upon metal coordination. This indicates that the direction of the coordination, at a substoichiometric amount of manganese ions, is in agreement with the formation of macrochelate systems, as found for multi-anchoring site peptides. Indeed, in all the obtained species, the Mn(II) ion is not able to induce amide deprotonation and coordination, thus the primary binding sites are not able to behave as an individual binding center with this metal ion.

At pH higher than 9 (Fig. 7), though a general broadening of all the signals can be seen, some specific shifts can be determined; in particular, the tyrosine chemical shifts of H $\epsilon$  and H $\delta$  were strongly affected, giving a  $\Delta\delta$  of 0.23 ppm (H $\epsilon$ )



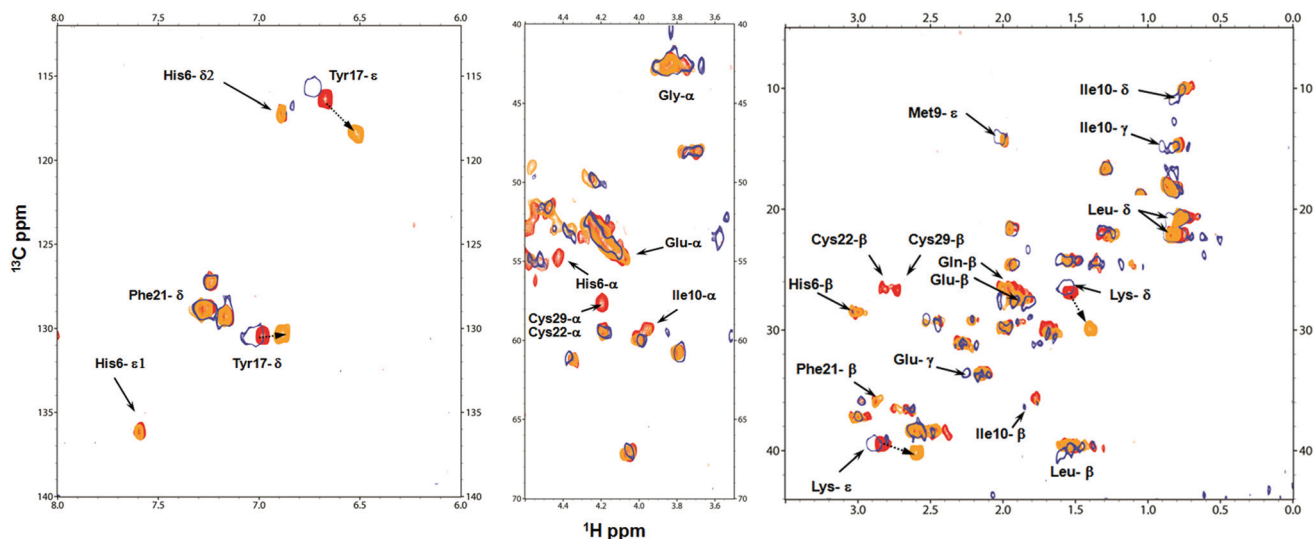


Fig. 7 Selection of aliphatic and aromatic regions in the  $^{13}\text{C}$ - $^1\text{H}$  HSQC NMR spectra for Park30 peptide, in the absence (red) and in the presence of 0.05 equivalent of  $\text{Mn}(\text{II})$ , at pH 9.2 (blue open circle) and pH 11.5 (orange).

and  $\Delta\delta$  of 0.20 ppm ( $\text{H}\delta$ ), from pH 9 to pH 11.5, which were similar to those obtained for the free ligand in the same range of pH, suggesting a deprotonation of the tyrosine oxygen which does not seem to be involved in the coordination.

EPR experiments have been performed at pH 7.5 and at pH 9 in a frozen solution at liquid nitrogen temperature as well as at room temperature in order to obtain some more information on the  $\text{Mn}(\text{II})$  coordination mode in the predominant species.

A typical EPR signal centered at around 3200 G ( $g$  around 2) splitted into six major hyperfine lines by the interaction of the unpaired electrons with the nuclear magnetic moment of  $^{55}\text{Mn}$  nucleus ( $I = 5/2$ , 100% natural abundance) and  $A$  around  $90 \times 10^{-4} \text{ cm}^{-1}$  and  $8 \times 10^{-4} \text{ cm}^{-1}$  of line width has been registered (Fig. S1†).

The obtained EPR spectra were very similar to those recorded for  $\text{Mn}(\text{H}_2\text{O})_6^{2+}$  ions under the same experimental conditions, indicating that in the  $\text{Mn}(\text{II})$ -Park30 species there is no significant deviation from an octahedral symmetry.

NMR results obtained within the pH range 7.5–9 and at a very low  $\text{Mn}(\text{II})$  to peptide molar ratio, dictated by the paramagnetism of the metal ion, are in agreement with the presence of a [2S,N,3O] chromophore from two cysteines, a histidine and three oxygens derived from glutamate and aspartate, resulting in a macrocycle environment, though it may be in equilibrium with species where manganese can be bound to all the oxygens present, derived from glutamic and aspartic residues.

By raising the pH over 9, possible variation in the oxidation state of manganese can happen as shown by the strong decrease in intensity of the paramagnetic EPR  $\text{Mn}(\text{II})$  signal.

In order to confirm the composition of the species formed in solution, mass spectrometry was also used. This method can be applied as a complementary technique to determine the metal to ligand stoichiometry directly from the  $m/z$  values. Analysis of the ESI-MS spectra of the reaction mixture of

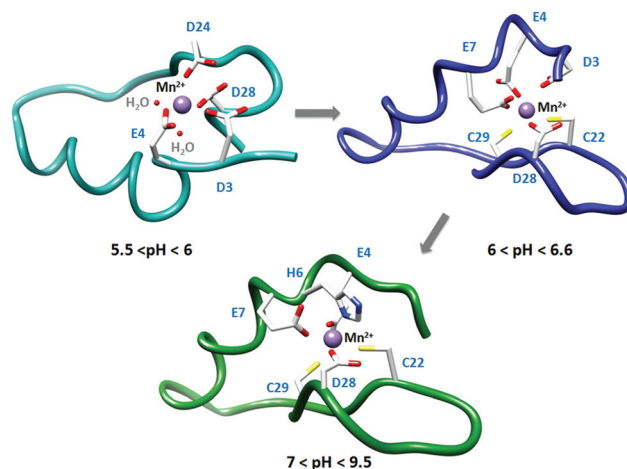


Fig. 8 Models of the most likely coordination spheres of the  $\text{Mn}(\text{II})$  ion in octahedral geometry with Park30 peptide at different pH values.

$\text{Mn}(\text{II})$ -Park30 with a metal to ligand molar ratio of 1:1.2 showed the formation of only monomeric species confirmed by the signal at  $m/z$  842.89, and assigned to the  $[\text{Mn}(\text{Park30})]^{4+}$  complex (Fig. S2†). A comparison between the experimental and simulated signals showed an excellent agreement.

The spectra recorded at pH 7.4 and 9.0 were identical.

Models of the most likely coordination spheres of the  $\text{Mn}(\text{II})$  ion in octahedral geometry with the Park30 fragment at different pH values are reported in Fig. 8.

### Zn(II) complexes

The potentiometric results reported in Table 3 were obtained from four titrations carried out with either HCl or NaOH between pH 5.5 and pH 11. No precipitation was observed in the alkaline pH range.

**Table 3** Complex-formation constants for the system Zn(II)/Park30, at  $T = 298\text{ K}$  and  $I = 0.1\text{ mol dm}^{-3}$  (KCl)

	$\log \beta$	$pK_a$
$[\text{ZnLH}_5]^{2-}$	54.6(3)	5.5
$[\text{ZnLH}_4]^{3-}$	49.07(8)	6.0
$[\text{ZnLH}_3]^{4-}$	43.1(2)	6.7
$[\text{ZnLH}_2]^{5-}$	36.42(9)	8.93
$[\text{ZnLH}]^{6-}$	27.49(5)	9.97
$[\text{ZnL}]^{7-}$	17.53(7)	10.2
$[\text{ZnLH}_{-1}]^{8-}$	7.3(1)	—

The comparison of titration curves registered in the absence or in the presence of Zn(II) (Fig. S3†) shows that, with equal volume of titrant added, the pH value is always lower for the solutions containing Zn(II), thus revealing the formation of complexes where the metal displaces some protons of the ligand. The formation of seven complexes of stoichiometry 1 : 1 (Zn(II) : peptide) was detected (Table 3 and Fig. 9). Potentiometry does not suggest the formation of any bis-complex. A small improvement of the degree of fitting can be instead obtained by inserting the complex  $[\text{Zn}_2\text{LH}_2]^{3-}$  into the speciation model, whose presence could be justified by the fact that one Zn(II) ion could bind the two cysteines in the C-terminal domain while, at the same time, another Zn(II) ion could bind the His residue, possibly assisted by Asp and Glu carboxylate side-chains, at the N-terminus. However, the calculated formation amount of this complex, under the conditions of an equimolar metal to ligand molar ratio used here, is too low to confirm its real existence. The prevalence of mono-complexes, confirmed also by ESI-MS measurements (Fig. S4†), is certainly favored by the metal to ligand ratio in solution (1 : 1.1), although it is worth underlining that this is not a sufficient condition: low, but not negligible, concentrations of complexes with stoichiometry other than 1 : 1 are normally formed even in equimolar solutions of metal and peptide, if the system allows it.

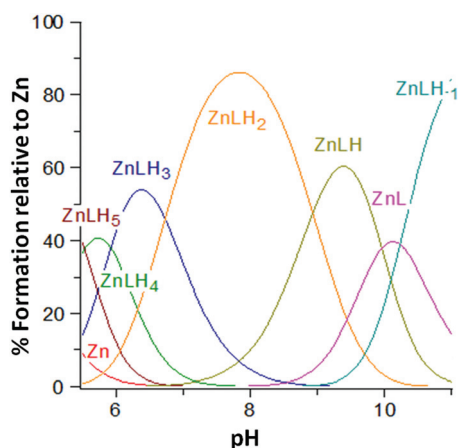


**Fig. 9** Representative distribution diagram for the complex-formation equilibria in the system Zn(II)/Park30;  $C_L^0 = 1 \times 10^{-3}\text{ mol dm}^{-3}$ ; M/L ratio = 1 : 1.

The presence in the speciation model of Table 3 of a species with stoichiometry  $[\text{ZnLH}_{-1}]^{8-}$  is also noteworthy: since the Zn(II) ion is not able to displace the amide protons of the peptide chain, it must be assumed that a proton from a water molecule bound to the metal has been released, to form a hydroxylated complex.

The first complex detected at the most acidic pH value is the species  $[\text{ZnLH}_5]^{2-}$  in which the anchoring site for zinc can be either a histidine or a cysteine. As a matter of fact, five sites of the peptide are protonated; among these, certainly are the two lysines and probably the tyrosine. Given the high affinity of zinc for the cysteines,<sup>12</sup> we can assume that in this complex both the sulfur atoms are already coordinated to the metal, forming a macrocycle. The other two coordination positions of the complex, most likely tetrahedral, may be occupied by water molecules, even if one cannot exclude the participation of one of the carboxylate groups available in the peptide. Under this hypothesis, the stoichiometry of the complex requires that both His and one of the two Glu residues are protonated. This hypothesis is supported by the results described in our previous report<sup>12</sup> where the stability of the zinc complexes formed by the two separate fragments of the peptide, PK9-H and PK9-C respectively, corresponding to the N- and C-terminal domains of Park30, is compared: the latter is a ligand stronger than the former in the whole pH range and it begins to form complexes at lower pH values.

Increasing the pH, two protons are released in a quick succession, to form first the species  $[\text{ZnLH}_4]^{3-}$  and then the complex  $[\text{ZnLH}_3]^{4-}$ ; the corresponding  $pK_a$  values (5.5 and 6.0, Table 3) are quite close to each other and can be attributed to the deprotonation of the glutamic acid ( $pK_a = 5.9$  in the absence of a metal, Table 1) and histidine ( $pK_a = 6.8$  in the absence of a metal, Table 1), the latter favored by the interaction with the metal center, *i.e.* to form a **hydrogen bond between the glutamate and a water molecule bound in the fourth position of the** tetrahedral structure [2S,N,O]. With the data available, one cannot accurately distinguish between these two processes, which take place almost simultaneously.

The prevailing species in a broad pH range around neutrality is the complex  $[\text{ZnLH}_2]^{5-}$ . The  $pK_a$  value corresponding to the loss of a proton from the complex  $[\text{ZnLH}_3]^{4-}$  (6.7, Table 3) is not compatible with the deprotonation of one lysine or tyrosine and could therefore be attributed to the release of a proton from a water molecule bound to zinc in the fourth coordination position of the tetrahedron. Therefore,  $[\text{ZnLH}_2]^{5-}$  should be a hydroxylated species, which should more correctly be written as  $[\text{ZnLH}_3(\text{OH})]^{5-}$  in order to highlight the presence of three protonated sites in the ligand and, at the same time, one hydroxyl ion bound to zinc.

Finally, in the alkaline pH range, the deprotonations of Tyr and of the two Lys residues can be observed, characterized by  $pK_a$  values of 8.9, 10.0 and 10.2, respectively (Table 3). Although such values are lower than those measured in the absence of a metal (9.5, 10.4, 10.5, Table 1), the formation of an additional coordination bond to the metal ion does not seem very likely since it would imply a change from tetrahedral to trigonal bipy-

amidal or octahedral coordination mode. Instead the NMR data (see below) suggest the replacement of histidine at very basic pH, probably by the phenolic residue of tyrosine.

Interaction of Zn(II) ions was evaluated by NMR techniques using a metal to ligand molar ratio of up to 1:1 over a pH range of 6–11.

Despite the low solubility of the peptide, at pH 5.5 and at a Zn(II) to peptide molar ratio of 1:1, the histidine and glutamic signals were clearly visible and not affected by zinc addition, thereby excluding binding of these residues in the coordination process.

At pH 6, H $\alpha$  and H $\beta$  protons of cysteines completely disappeared from the spectra. Some minor changes in the chemical shifts of H $\alpha$  and H $\beta$  protons of Cys29, and to a lesser extent of Cys22, were observed in the HSQC spectra. Some loss in the signal intensity was detected for Asp residues although it was not possible to identify the specific residue involved.

Overall, the most apparent feature emerging from the 1D, TOCSY and HSQC spectra was the general decrease in the intensity of all signals, particularly those that could be selectively correlated to cysteines, Cys22 and Cys29, histidine His6 as well as glutamic, Glu4 and Glu7 residues.

The general loss in intensity of the NMR signals can be ascribed to several causes, the most plausible one in our study being the presence of chemical exchange between various conformational states in an intermediate regime with respect to the NMR timescale, derived from the multitude of binding sites within the Park30 sequence.

Some additional information was obtained using a metal to ligand molar ratio of 0.75:1 in the range of pH 7.3–11.5.

Small changes in the chemical shifts of  $\alpha$  nuclei were detected for the closest residues to the binding center Ala26, Asp27 together with Met9 and Ile10 and Tyr17 supporting changes in the backbone conformation as expected upon metal coordination.

In fact, in the HSQC spectra obtained at pH 7.5 the disappearance of H $\beta$  of His6 together with a shift of H $\beta$  and H $\alpha$  from both cysteine residues, Cys22 and Cys29 were clearly observable.

In Fig. 10 the histogram of the detected changes of proton and carbon chemical shifts in the NMR spectra after zinc coordination is reported.

When the pH value was raised to 8.6, the shifts involving H $\delta$ 2 and H $\epsilon$ 1 of the histidine residue became even more apparent, suggesting that cysteine residues act as primary anchoring sites for Zn(II) coordination. The histidine residue was also involved in Zn(II) coordination, forming different macrocycles which can coexist in a dynamic equilibrium.

At pH 8.6, H $\delta$ 2 and H $\epsilon$ 1 signals from histidine move towards lower fields, showing that the chemical environment of histidine has undergone a change after coordination. At higher pH no more changes have been detected.

At pH 11, a reappearance of the histidine signals as in the free ligand has been evidenced suggesting that at very high pH histidine cannot be involved in the coordination with the Zn(II) ion.

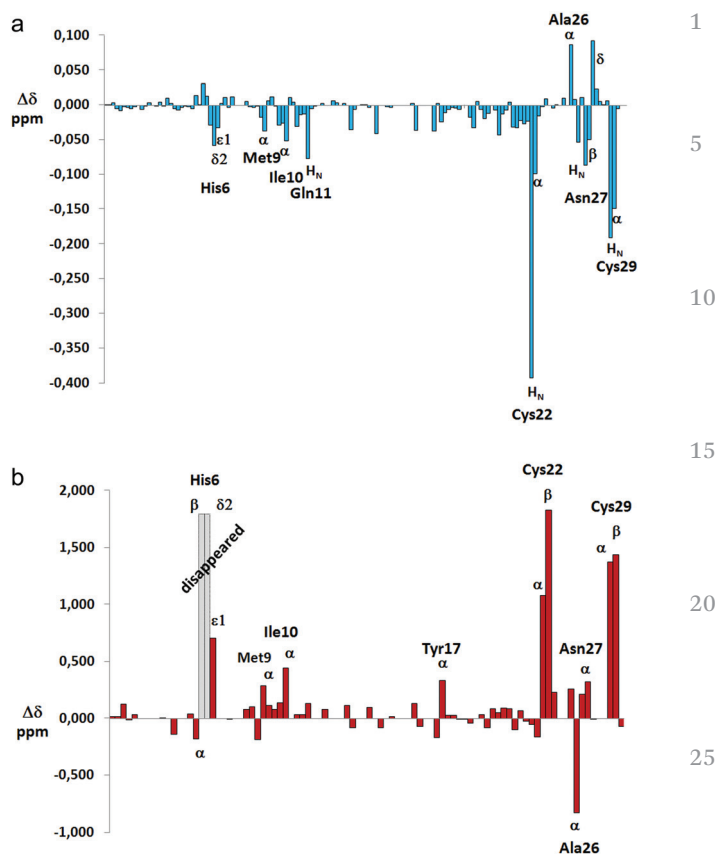


Fig. 10 Plot of the observed  $^1\text{H}$  proton (a) and  $^{13}\text{C}$  carbon (b) chemical shift changes ( $\Delta\delta = \delta_{\text{Zn}} - \delta_{\text{free}}$ ) for Park30 peptide following Zn(II) coordination at pH 7.3.

## Conclusions

In this paper we described the interaction of Mn(II) and Zn(II) ions with a Park30 sequence which is characterized by the presence of multiple metal binding sites. In particular, the occurrence of multi-anchoring sites for Mn(II) and Zn(II) borderline metal ions was responsible for the wide structural variety of the obtainable complexes, also depending on the metal to ligand molar ratio.

In fact, it is known that the multiple sites could serve as independent binding sites for metal ions or, a single metal ion could bind all or almost all of the sites, as dictated by the used conditions or metal geometrical requirements. Indeed, the presence of two cysteine residues and one histidine residue within the sequence may lead to the formation of macrochelates since both metal ions Mn(II) and Zn(II) bound by the peptide are incapable of deprotonating amide nitrogens from the backbone and, in particular, the formation of macrocycles is driven by the oxygen donor atoms that are present within the sequence.

The primary binding sites for the coordination of Zn(II) ions resulted in two cysteine residues (Cys22 and Cys29) followed by a histidine residue (His6) with the involvement of a

[2S,N,2O] chromophore in a possible tetrahedral arrangement at physiological pH.

The predominant species for the Mn(II) ion was a [2S,N,3O] chromophore only at a very low metal to ligand molar ratio, whereas at a metal to ligand molar ratio of 1:1 the experimental data converge on a structural hypothesis of coordinated species presumably octahedral in which the Mn(II) ion is mainly bound to the oxygens of the carboxylate groups of the peptide, and possibly also to some water molecules.

Interestingly, binding within the Park30 sequence would seem to be less definite than what was observed in a previous study for the shorter PK9-H and PK9-C fragments and a dynamic exchange of different coordination modes cannot be neglected.

When comparing the metal binding ability of different peptides, many factors should be taken into account; for example, the metal concentration in the cytosol should be not high enough to trigger a selective response, or metals do not elicit the required coordination number or geometry.

In Table 4 are reported  $K_d$  and pM values for Mn/Zn-Park30 species and for Mn/Zn-PK9-C, Mn/Zn-PK9-H<sup>12</sup> and Mn/prion protein,<sup>31</sup> for the sake of comparison. First of all, it is possible to note that Mn(II) complexes of Park30 are characterized by a  $K_d$  value slightly lower but comparable to that reported for the prion protein. In addition, Mn(II) and Zn(II) complexes with Park30 fragments are much more stable than those with the smaller PK9-C and PK9-H fragments. The same conclusion can be clearly deduced from the competition diagrams shown in Fig. S5–S8 (ESI†) which show that Park30 dominates over the short fragments throughout all the pH range. The presence of multiple binding sites in the Park30 fragment allows the formation of a high number of different isomeric complexes with the same stoichiometry, most likely extra-stabilized by additional intra-molecular interactions among the side chains of the amino acid residues. This can be the reason why the long peptide can form complexes with a higher stability.

Moreover, such binding behavior suggests that the entire protein, having a large number of coordinating residues, especially those bearing oxygen donors such as Asp or Glu resi-

**Table 4** Dissociation constant  $K_d$  and pM values for Zn(II) and Mn(II) complexes with PK9-H,<sup>12</sup> PK9-C,<sup>12</sup> Park30 peptides (at pH 7.4) and prion protein<sup>31</sup> (at pH 5.5)

System	$K_d/M^{-1}$	pM
Zn(II)/Park30	$2.38 \times 10^{-11}$	10.9
Mn(II)/Park30	$2.34 \times 10^{-6}$	6.7
Mn(II)/Park30 <sup>a</sup>	$12.5 \times 10^{-6}$	
Mn(II)/Prion protein <sup>a</sup>	$63\text{--}200 \times 10^{-6}$	
Zn(II)/PK9-H	$4.61 \times 10^{-4}$	6.01
Zn(II)/PK9-C	$4.63 \times 10^{-9}$	7.35
Mn(II)/PK9-H	$5.69 \times 10^{-4}$	6.01
Mn(II)/PK9-C	$8.09 \times 10^{-4}$	6.01

<sup>a</sup> pH 5.5.

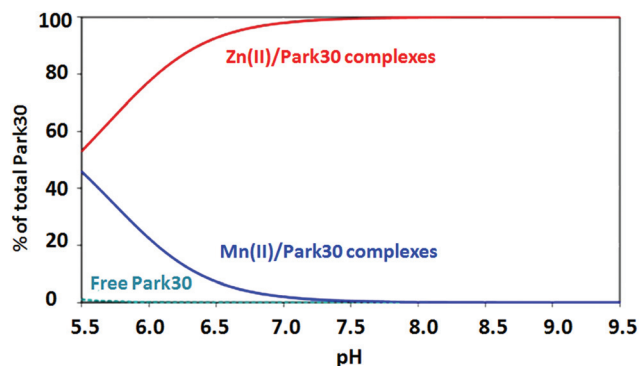


**Fig. 11** Representative competition diagrams for a binary solution containing the metal ion (either Mn(II) or Zn(II)) and Park30 ligand.

dues, may play a crucial role in sequestering, carrying or possibly oxidizing the bound metal ions and indeed makes it possible to attribute a role to the Park9 protein in metal detoxification.

Potentiometric data reveal that the affinity of Park30 for Zn(II) is much higher than that for Mn(II) (see Table 4): at physiological pH and equimolar concentrations of the three reagents, Park30 is totally involved in Zn(II) complexes (see competition diagram in Fig. 11). However Mn(II) can compete with Zn(II) ions for the binding at acidic pH: under the simulated conditions, at pH 5.5, the Park30 fragment is shared between Zn(II) and Mn(II) at about 50% (Fig. 11).

Therefore, if we consider that Glu and Asp residues are already deprotonated at low pH values and that, like in prion protein,<sup>31</sup> Mn(II) is capable of binding oxygens at pH 5.5, then, it is quite possible that the Park9 (YPk9) protein may possess a striking ability for binding manganese, which can also compete with other metal ions at pH values as low as those observed within the vacuole, where the protein is mainly localized.

## Acknowledgements

The financial support of the University of Ferrara (FAR 2014) is gratefully acknowledged. We also gratefully acknowledge financial support from Regione Autonoma Sardegna L.R.7/2007, “Promozione della ricerca scientifica e dell’innovazione tecnologica in Sardegna” program, project CRP 26712 “Metallic nanoparticles: the real cause of Quirra syndrome?”.

## References

- C. L. Keen, J. L. Ensunsa and M. S. Clegg, *Met. Ions Biol. Syst.*, 2000, **37**, 89–121.
- M. A. Zoroddu, S. Medici, A. Ledda, V. M. Nurchi, J. I. Lachowicz and M. Peana, *Curr. Med. Chem.*, 2014, **21**, 3837–3853.



- 1 3 J. Crossgrove and W. Zheng, *NMR Biomed.*, 2004, **17**, 544–553.
- 4 S. L. O’Neal and W. Zheng, *Curr. Environ. Health Rep.*, 2015, **2**, 315–328.
- 5 5 M. Aschner, T. R. Guilarte, J. S. Schneider and W. Zheng, *Toxicol. Appl. Pharmacol.*, 2007, **221**, 131–147.
- 6 C. Au, A. Benedetto and M. Aschner, *Neurotoxicology*, 2008, **29**, 569–576.
- 10 7 R. Squitti, G. Gorgone, V. Panetta, R. Lucchini, S. Bucossi, E. Albini, L. Alessio, A. Alberici, J. M. Melgari, L. Benussi, G. Binetti, P. M. Rossini and F. Draicchio, *J. Neural Transm.*, 2009, **116**, 1281–1287.
- 8 D. P. Perl and C. W. Olanow, *J. Neuropathol. Exp. Neurol.*, 2007, **66**, 675–682.
- 15 9 P. Zhang, K. M. Lokuta, D. E. Turner and B. Liu, *J. Neurochem.*, 2010, **112**, 434–443.
- 10 A. D. Gitler, A. Chesi, M. L. Geddie, K. E. Strathearn, S. Hamamichi, K. J. Hill, K. A. Caldwell, G. A. Caldwell, A. A. Cooper, J. C. Rochet and S. Lindquist, *Nat. Genet.*, 2009, **41**, 308–315.
- 20 11 S. Medici, M. Peana, L. G. Delogu and M. A. Zoroddu, *Dalton Trans.*, 2012, **41**, 4378–4388.
- 12 M. Remelli, M. Peana, S. Medici, L. G. Delogu and M. A. Zoroddu, *Dalton Trans.*, 2013, **42**, 5964–5974.
- 25 13 P. Gans, A. Sabatini and A. Vacca, *Talanta*, 1996, **43**, 1739–1753.
- 14 L. Alderighi, P. Gans, A. Ienco, D. Peters, A. Sabatini and A. Vacca, *Coord. Chem. Rev.*, 1999, **184**, 311–318.
- 30 15 H. Kozlowski, M. Luczkowski and M. Remelli, *Dalton Trans.*, 2010, **39**, 6371–6385.
- 16 G. Crisponi and M. Remelli, *Coord. Chem. Rev.*, 2008, **252**, 1225–1240.
- 17 M. A. Zoroddu, M. Peana and S. Medici, *Dalton Trans.*, 2007, 379–384.
- 18 M. A. Zoroddu, S. Medici, M. Peana and R. Anedda, *Dalton Trans.*, 2010, **39**, 1282–1294.
- 19 M. Peana, S. Medici, V. M. Nurchi, G. Crisponi and M. A. Zoroddu, *Coord. Chem. Rev.*, 2013, **257**, 2737–2751.
- 20 M. A. Zoroddu, T. Kowalik-Jankowska, S. Medici, M. Peana and H. Kozlowski, *Dalton Trans.*, 2008, 6127–6134.
- 21 M. A. Zoroddu, M. Peana, S. Medici, S. Potocki and H. Kozlowski, *Dalton Trans.*, 2014, **43**, 2764–2771.
- 22 M. A. Zoroddu, M. Peana, S. Medici and R. Anedda, *Dalton Trans.*, 2009, 5523–5534.
- 23 C. Lambert, N. Leonard, X. De Bolle and E. Depiereux, *Bioinformatics*, 2002, **18**, 1250–1256.
- 24 J. P. Morth, B. P. Pedersen, M. S. Toustrup-Jensen, T. L. Sorensen, J. Petersen, J. P. Andersen, B. Vilsen and P. Nissen, *Nature*, 2007, **450**, 1043–1049.
- 25 M. Peana, S. Medici, V. M. Nurchi, G. Crisponi, J. I. Lachowicz and M. A. Zoroddu, *Dalton Trans.*, 2013, **42**, 16293–16301.
- 26 E. F. Pettersen, T. D. Goddard, C. C. Huang, G. S. Couch, D. M. Greenblatt, E. C. Meng and T. E. Ferrin, *J. Comput. Chem.*, 2004, **25**, 1605–1612.
- 27 H. Sigel and R. B. Martin, *Chem. Rev.*, 1982, **82**, 385–426.
- 28 L. D. Pettit and K. Powell, Royal Society of Chemistry, London, 1992–2000. **Q4**
- 29 H. M. Irving, M. G. Miles and L. D. Pettit, *Anal. Chim. Acta*, 1967, **38**, 475–488.
- 30 J. D. Crowley, D. A. Traynor and D. C. Weatherburn, *Met. Ions Biol. Syst.*, 2000, **37**, 209–278.
- 31 M. W. Brazier, P. Davies, E. Player, F. Marken, J. H. Viles and D. R. Brown, *J. Biol. Chem.*, 2008, **283**, 12831–12839.